Nucleic Acids Research, 2023, **51**, 10815–10828
https://doi.org/10.1093/nar/gkad861
Advance access publication date: 20 October 2023
NAR Breakthrough Article

An ATP-independent role for Prp16 in promoting aberrant splicing

Che-Sheng Chung, Hsu Lei Wai, Ching-Yang Kao and Soo-Chen Cheng *

Institute of Molecular Biology, Academia Sinica, Taipei, Taiwan 115, Republic of China

*To whom correspondence should be addressed. Tel: +886 2 27899200; Fax: +886 2 27883296; Email: mbscc@ccvax.sinica.edu.tw
Present addresses:
Hsu Lei Wai, Department of Chemistry, Biochemistry and Pharmaceutical Sciences, University of Bern, 3012 Bern, Switzerland.
Ching-Yang Kao, Center for Frontier Medicine, National Taiwan University Hospital, Taipei, Taiwan 100, Republic of China.

Abstract

The spliceosome is assembled through a step-wise process of binding and release of its components to and from the pre-mRNA. The remodeling process is facilitated by eight DExD/H-box RNA helicases, some of which have also been implicated in splicing fidelity control. In this study, we unveil a contrasting role for the prototypic splicing proofreader, Prp16, in promoting the utilization of aberrant 5′ splice sites and mutated branchpoints. Prp16 is not essential for the branching reaction in wild-type pre-mRNA. However, when a mutation is present at the 5′ splice site or if Cwc24 is absent, Prp16 facilitates the reaction and encourages aberrant 5′ splice site usage independently of ATP. Prp16 also promotes the utilization of mutated branchpoints while preventing the use of nearby cryptic branch sites. Our study demonstrates that Prp16 can either enhance or impede the utilization of faulty splice sites by stabilizing or destabilizing interactions with other splicing components. Thus, Prp16 exerts dual roles in 5′ splice site and branch site selection, via ATP-dependent and ATP-independent activities. Furthermore, we provide evidence that these functions of Prp16 are mediated through the step-one factor Cwc25.

Graphical abstract

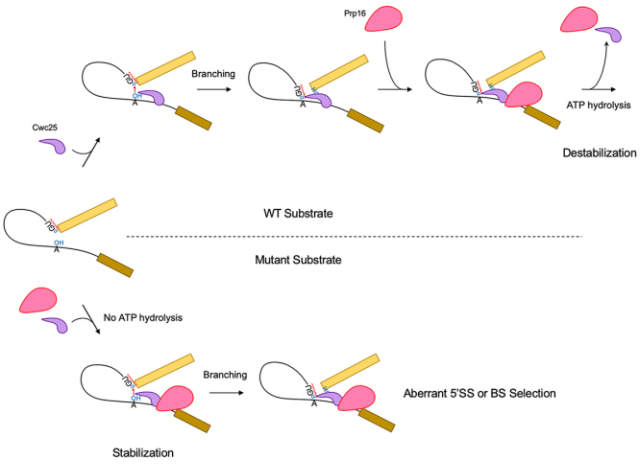

Introduction

Splicing of precursor mRNA occurs via two consecutive steps of a transesterification reaction that are catalyzed by the spliceosome. Composed of five small nuclear RNAs—U1, U2, U4/U6 and U5—and numerous protein factors (1,2), the spliceosome is assembled in a step-wise manner by binding of small nuclear ribonucleoprotein particles (snRNPs) to specific sites within the pre-mRNA in the order of U1, U2 and then the U4/U6·U5 tri-snRNP (3–6). Spliceosome assembly predominantly commences with binding of U1 to the 5′ splice site (5′SS) and U2 to the branch site (BS), forming the pre-spliceosome. Following addition of the tri-snRNP, the spliceosome undergoes a major structural change by releasing U1 and U4 and incorporating the Prp19-associated complex, also known as NTC (nineteen complex) (7–9). This conformational change results in a rearrangement of RNA interactions, generating an RNA-based catalytic center that catalyzes the splicing reaction (10,11). The splicing reaction occurs in two transesterification steps, cleavage at the 5′SS and formation of the lariat intron–exon 2 in the first step (referred to as 5′SS cleavage or branching later in the text) and cleavage of the 3′ splice site (3′SS) and ligation of the two exons in the second step (referred to as exon ligation).

Received: June 30, 2023. **Revised:** September 3, 2023. **Editorial Decision:** September 5, 2023. **Accepted:** September 23, 2023

Structural changes of the spliceosome involve the formation and disruption of RNA–RNA, RNA–protein and protein–protein interactions, mediated by members of DExD/H-box RNA helicases (12–14). In the yeast *Saccharomyces cerevisiae*, the entire splicing process involves eight DExD/H-box proteins, two of which, Prp2 and Prp16, are required for the catalytic step (14–17). Although the RNA catalytic center has formed by the time the spliceosome is activated, the branch helix is still 50 Å away from the 5′SS, separated by SF3B1, a component of the U2 snRNP SF3b subcomplex (18). Prp2 acts to destabilize SF3a/b so that the BS can be positioned into the catalytic center adjacent to the 5′SS. Consequently, a binding site for Cwc25 is generated, which is crucial for promoting the branching reaction, presumably by stabilizing the interaction between the 5′SS and the BS (19,20). Following the branching reaction, Cwc25 becomes tightly associated with the spliceosome, occupying the catalytic center along with Yju2. To enable positioning of the 3′SS for exon ligation, Yju2 and Cwc25 then must vacate the catalytic center. Prp16 mediates the release of Yju2 and Cwc25 after branching (17), and is not required for the branching reaction (16).

PRP16 was initially identified as a suppressor of branchpoint (BP) A-to-C mutation (brC) in a genetic screen for BS-binding proteins. Prp16 mutants with reduced ATPase activity were found to increase the splicing efficiency of brC pre-mRNA (21,22), leading to the hypothesis that Prp16 plays a role in ensuring splicing fidelity through ATP hydrolysis by discriminating against BP mutations after branch formation (21–23). Prp16 has also been implicated in proofreading slow 5′SS cleavage (24), and so it may proofread both the 5′SS and the BS sequences. Beyond its role in proofreading the splice sites, Prp16 has also been demonstrated to promote utilization of alternative branch sites when branchpoint A (brA) is replaced with deoxyA (d-brA) (25).

Although Prp16 is dispensable for the branching reaction during splicing of wild-type pre-mRNA (16), it has been shown to facilitate the branching reaction of BP-mutated pre-mRNAs through an ATP-independent mechanism (17). Upon catalytic activation of the spliceosome, Cwc25 binds to the spliceosome and promotes the branching reaction. However, the interaction is compromised when a mutation occurs at the BP. The presence of Prp16, especially the ATPase mutant of Prp16, stabilizes the interaction, thereby promoting branching. Conversely, the ATPase activity of Prp16 can also facilitate the removal of Cwc25 before the branching reaction takes place. This dynamic suggests that the ATPase function of Prp16, which destabilizes Cwc25 prior to branching, competes with the ATP-independent function of Prp16, which stabilizes Cwc25, ultimately dictating the branching efficiency of BP-mutated pre-mRNA. Accordingly, reducing the ATPase activity of Prp16 enables more splicing of BP mutants. This interpretation offers an alternative explanation for the genetic suppression of the brC mutation by Prp16 ATPase mutants (17).

In this study, we show that the ATP-independent function of Prp16 also promotes aberrant 5′SS cleavage. Specifically, when a pre-mRNA carries a G5A mutation at the 5′SS or when splicing is performed in the absence of step-one factor Cwc24, which normally binds to the 5′SS, splicing is predominantly inhibited, albeit with a low level of leak-through activity that also generates a shorter 5′ exon (5Ex) due to cleavage at the –5 position of the 5Ex (26). We show that depletion of Prp16 inhibits cleavage at the aberrant site in both those cases. Using the G5A mutant pre-mRNA to explore the underlying mechanism, we found that the G5A mutation greatly weakened the interactions of Prp8 with the 5′SS. Although cleavage of G5A pre-mRNA at the authentic 5′SS occurs at a faster rate than at alternative sites, the reaction is limited in the presence or absence of Prp16. In contrast, cleavage at aberrant sites proceeds slowly but steadily over time in the presence of Prp16. We propose that the 5Ex of the G5A mutant pre-mRNA only interacts dynamically with Prp8, as it is not stably clamped by Prp8. This dynamic interaction prevents proper interaction of the BP with the 5′SS. Binding of Prp16 stabilizes this interaction, promoting branching but with reduced specificity, resulting in cleavage at aberrant sites. We also show that Prp16 prevents the utilization of a cryptic branch site (CBS) in splicing of brC and brG pre-mRNAs, enabling the mutated nucleotides to serve as the sole BP. Our results reveal that the ATP-dependent and ATP-independent functions of Prp16 play contradictory roles in controlling splicing fidelity. More specifically, the ATPase activity of Prp16 prevents the usage of mutated splice sites, whereas the ATP-independent function of Prp16 facilitates the usage of mutated BP or aberrant 5′SS by stabilizing Cwc25's interaction with the spliceosome. This scenario raises doubts about whether Prp16 is actively involved in proofreading splice sites.

Materials and methods

Yeast strains

The following yeast strains were used: BJ2168 (MATa prc1 prb1 pep4 leu2 trp1 ura3); YSCC037 (MATa prc1 prb1 pep4 leu2 trp1 V5-CWC24); YSCC038 (MATa prc1 prb1 pep4 leu2 trp1 GAL1-CWC24::URA3); YSCC256 (MATa prc1 prb1 pep4 leu2 trp1 CWC25-V5); and SS304 (MATa prp2-1 ade1 ade2 ura1 his7 typ1 lys2 gal1).

Antibodies and reagents

Anti-hemagglutinin (anti-HA) monoclonal antibody 8G5F was produced by immunizing mice with a keyhole limpet hemocyanin (KLH)-conjugated HA peptide. Anti-V5 monoclonal antibody was purchased from Serotec Inc. Anti-Prp16 and anti-Ntc20 antibodies were raised by injecting rabbits with recombinant proteins of amino acids 1–298 for Prp16 and of full-length protein for Ntc20, respectively. Protein A–Sepharose (PAS) was obtained from GE Healthcare Inc. Proteinase K was purchased from Cyrusbioscience Inc. RNA oligos and dinucleotide 4sUpG were purchased from Dharmacon.

Oligonucleotides

Oligonucleotides used for the construction of plasmids and for synthesizing the various substrates are listed in the Supplementary Materials and methods.

Construction of plasmids

Procedures for the construction of plasmids are described in the Supplementary Materials and Methods.

Preparation of splicing extracts and substrates

Yeast whole-cell extracts were prepared according to the method described in Cheng *et al*. (27). Extracts metabolically depleted of Cwc24 were prepared as described in Wu *et al*.

(26). Splicing substrates were synthesized by *in vitro* transcription with SP6 RNA polymerase using EcoRI-linearized pSPAct6-88 plasmid and its derivatives as templates. 4sU-labeled pre-mRNAs were prepared according to the procedure described in Chung *et al*. (28) with some modifications. Each 4sU-labeled pre-mRNA was generated by ligation of three RNA fragments in two steps. The very 5′-RNA fragment (L), generated by SP6 RNA polymerase synthesis, was first ligated with an RNA oligo (M). The ligated product (5′) was purified by electrophoresis on a 7% denaturing polyacrylamide gel, and further ligated with the 3′ fragment (3′) primed with 4sUpG at the 5′ end, which was synthesized using SP6 RNA polymerase and labeled at its 5′ end with ^{32}P. The ligated pre-mRNA was purified by electrophoresis on a 5% denaturing polyacrylamide gel. The pre-mRNA with 2′-deoxyA labeling at the BP position was also generated by one-step three-fragment ligation of the 5′ fragment, an RNA oligo containing deoxyA and the 3′ fragment, together with a DNA splint, at a ratio of 4:2:4:3 according to the procedure described in Chung *et al*. (28).

In vitro splicing assay, immunodepletion and immunoprecipitation of the spliceosome

Splicing assays were carried out according to the procedure described in Cheng *et al*. (27) at 25°C for 30 min using 40% (v/v) regular extracts or 50% (v/v) immunodepleted extracts unless otherwise indicated. For cross-linking analyses, splicing reactions were carried out in a 20 μl reaction volume with 0.4 nM 4sU-labeled V3 pre-mRNA, or in a 60 μl reaction volume with 1.2 nM 4sU-labeled V3-G5A pre-mRNA.

Immunoprecipitation of the spliceosome was performed as described (8). For each 10–20 μl of splicing reaction mixture, we used 10 μl of PAS conjugated with 1.5 μl of anti-Ntc20, 1 μl of anti-Prp8 or 5 μl of anti-Ntc30 antibody. To precipitate V5-tagged Cwc25, Prp8, Yju2 or Cwc24, 1 μl of anti-V5 antibody was used. To precipitate Ntc30-HA, we used 1 μl of anti-HA antibody. For Prp16 depletion, 100 μl of yeast extracts was incubated with 50 μl of PAS conjugated with 50 μl of anti-Prp16 antibody, at 4°C for 1 h, and the supernatant was collected after centrifugation.

Cross-linking with 4sU-labeled pre-mRNA

Site-specific 4sU cross-linking was performed according to Chung *et al*. (28) with some modifications. The reaction mixtures were placed as drops on a pre-cooled Parafilm-covered aluminum block and irradiated with $UV_{365\ nm}$ for 10 min at a distance of ∼3 cm from the UV lamp in a CL-1000 Ultraviolet Crosslinker system (UVP). For V3 pre-mRNA, each 20 μl of the irradiated reaction mixture was precipitated with 10 μl of PAS conjugated with 1.5 μl of anti-Ntc20 antibody, and the spliceosome-bound PAS was further washed with NET-2 buffer (50 mM Tris–HCl pH 7.4, 150 mM NaCl, 0.05% NP-40). For V3-G5A pre-mRNA, 60 μl of the irradiated reaction mixture was precipitated with 15 μl of PAS conjugated with 6 μl of anti-Ntc20 antibody, and the spliceosome-bound PAS was further washed with NET-2–300 (50 mM Tris–HCl pH 7.4, 300 mM NaCl, 0.05% NP-40). The washed precipitates were incubated with an equal volume of solution containing 0.06 U/μl Nuclease P1 and 6× Complete EDTA-free protease inhibitor cocktail at 37°C for 30 min. Proteins were analyzed by sodium dodecylsulfate–polyacrylamide gel electrophoresis (SDS–PAGE). To identify specific proteins, the irradiated mixtures were treated with Nuclease P1 as described above and then denatured in the presence of 1% SDS, 1% Triton X-100 and 100 mM dithiothreitiol (DTT) in boiling water for 90 s. The mixtures were diluted 10-fold with NET-2–300 and subjected to immunoprecipitation. The precipitates were treated with Nuclease P1 again and analyzed by SDS–PAGE.

Primer extension

Primer extension was performed with SuperScript III reverse transcriptase based on the method described in Chan *et al*. (29) using the indicated primers. Extension products were analyzed by electrophoresis on 10% polyacrylamide/8 M urea gels.

Quantification

Gels were exposed to IMAGING PLATE (FUJIFILM Corp.). RNA bands were quantified with a Typhoon™ FLA 9000 system (GE Healthcare Life Sciences) and analyzed using ImageQuant TL7.0 (GE Healthcare Life Sciences). The value of each quantified RNA band was normalized to the number of uridines in each RNA species to obtain relative molecular amounts.

Results

PRP16 promotes aberrant 5′ splice site cleavage

By proofreading the BS sequence and activating alternative BSs, Prp16 exerts multiple functions in the splicing reaction (25,30). Prp16 has also been implicated in proofreading 5′SS cleavage, leading to the rejection of slow spliceosomes (24). To gain deeper insights into the role of Prp16 in proofreading the 5′SS, we investigated its effect on splicing *ACT1* pre-mRNA carrying a G5A mutation at the 5′SS (Figure 1A), which has been shown previously to result in aberrant 5′SS cleavage (26,31). Splicing of the G5A pre-mRNA produced only minimal amounts of products (Figure 1B, lanes 3, 5, 7 and 9), with this outcome being more apparent upon spliceosome enrichment by precipitation with anti-Ntc20 antibody (Figure 1B, lanes 4, 6, 8 and 10). As expected, the generated 5Ex was smaller than that from wild-type pre-mRNA (Figure 1B, lane 4). Surprisingly, the size of the 5Ex was normal when Prp16 was depleted from the extract using a polyclonal antibody against Prp16 (Figure 1B, lane 6). Primer extension analysis confirmed that the cleavage site was the same as for wild-type pre-mRNA (Figure 1C, lanes 1 and 3), in contrast to cleavage occurring at the –5 position of the 5Ex in the presence of Prp16 (Figure 1C, lane 2). Interestingly, both normal and aberrant 5Exs were generated when an ATPase mutant of Prp16 (D473A) was added to the reaction (Figure 1B, lane 10). Notably, the spliced product (IVS, intervening sequence) was detected in the presence of wild-type (Figure 1B, lanes 4 and 8) but not mutant Prp16 (Figure 1B, lane 10). We reasoned that in the presence of wild-type Prp16, the aberrant 5Ex might be prevented from exon ligation, whereas the normal 5Ex could be ligated to form mRNA. With the D473A mutant, both normal and aberrant 5Ex were detected when splicing was blocked for exon ligation. Therefore, we mutated the 3′SS (ACAC) of the G5A pre-mRNA to block exon ligation (Figure 1D), and found that indeed both normal and aberrant 5Ex were generated in the presence of wild-type Prp16 (Figure 1D, lanes 1, 2 and 5). Consistent with those results, amounts of aberrant 5Ex were significantly reduced in the absence of

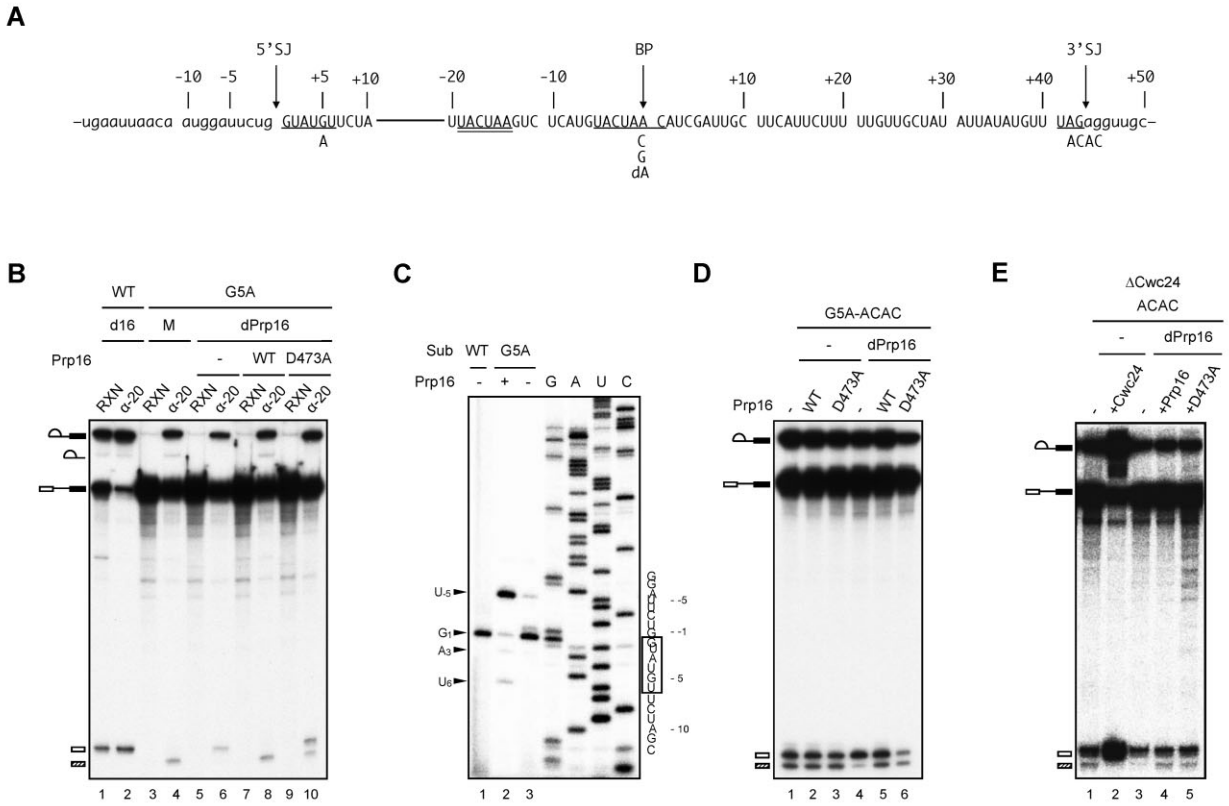

Figure 1. Prp16 promotes ATP-independent aberrant 5′ splice site cleavage of *ACT1* G5A pre-mRNA or wild-type pre-mRNA in Cwc24-depleted extracts. (**A**) The sequence of *ACT1* pre-mRNA is depicted in the 5′SS and BS–3′SS regions. Intron sequences are represented in upper case letters, and exons in lower case letters. Conserved splice site sequences are underlined. The CBS is double underlined. Mutations utilized in this study, including G5A at the 5′SS, brC and brG at the BS and ACAC at the 3′SS, are indicated. The 5′SJ and the BP are assigned as coordinate 0 for the 5′SS and the BS, respectively. 5′SJ, 5′ splice junction; 3′SJ, 3′ splice junction; BP, branchpoint. (**B**) Splicing was performed in Prp16-depleted extracts (lanes 1, 2 and 5–10), without (lanes 1, 2, 5 and 6) or supplemented with wild-type Prp16 (lanes 7 and 8) or the D473A mutant (lanes 9 and 10), or mock-treated extracts (lanes 3 and 4) using wild-type (lanes 1 and 2) or G5A mutant (lanes 3–10) pre-mRNA. The reaction mixtures were precipitated with anti-Ntc20 antibody. The striated rectangle denotes aberrant 5Ex. RXN, 1/10 of reaction mix; d16, Prp16 depletion; α-20, anti-Ntc20; Sub, substrate. (**C**) Primer extension using ACT1-A6 primer to map the 5′ cleavage site of wild-type (lane 1) or G5A (lanes 2 and 3) pre-mRNA in the absence (lanes 1 and 3) or presence (lane 2) of Prp16. The 5′SS sequence is boxed. (**D**) Splicing of *ACT1* G5A-ACAC pre-mRNA in extracts without (lanes 1–3) or with (lanes 4–6) prior depletion of Prp16 and without (lanes 1 and 4) or supplemented with wild-type Prp16 (lanes 2 and 5) or the D473A mutant (lanes 3 and 6). The reactions mixtures were precipitated with anti-Ntc20 antibodies. The striated rectangle denotes aberrant 5Ex. (**E**) Splicing of *ACT1* ACAC pre-mRNA in ΔCwc24 extracts without (lanes 1–2) or with (lanes 3–5) prior depletion of Prp16 and supplemented with Cwc24 (lane 2) or with wild-type Prp16 (lane 4) or the D473A mutant (lane 5). The reaction mixtures were precipitated with anti-Ntc20 antibody. The striated rectangle denotes aberrant 5Ex.

Prp16 (Figure 1D, lane 4). These results indicate that Prp16 promotes cleavage of G5A pre-mRNA at the aberrant 5′SS in addition to directing the spliceosome towards the discard pathway.

We have demonstrated previously that splicing of wild-type pre-mRNA in extracts depleted of the step-one factor Cwc24 also results in the generation of aberrant 5Ex due to cleavage at the –5 position on the 5Ex (26). Thus, using ACAC pre-mRNA, we examined if aberrant 5′SS cleavage in Cwc24-depleted extracts also requires Prp16 (Figure 1E). Similar to our findings for splicing of G5A pre-mRNA, depletion of Prp16 from extracts metabolically depleted of Cwc24 led to a significantly lower level of aberrant 5Ex (Figure 1E, lane 3), whereas the D473A mutant yielded similar levels to those found for wild-type Prp16 (Figure 1E, lanes 4 and 5). Therefore, Prp16 promotes aberrant 5′SS cleavage of both 5′SS-mutated pre-mRNA and wild-type pre-mRNA in Cwc24-depleted extracts, and this function is ATP independent. To rule out the possibility of substrate specificity for Prp16-mediated aberrant 5′SS cleavage, we analyzed the splicing of two other pre-mRNAs, i.e. *RPS6A* and *RPL23A* that harbor a G5A mutation in the introns and an AC mutation at the 3′SS to block exon ligation (Supplementary Figure S1). In both cases, the presence of Prp16 increased the ratio of aberrant to normal 5Ex (Supplementary Figure S1B). Thus, the function of Prp16 in promoting aberrant 5′SS cleavage of the G5A mutant pre-mRNA is not specific to *ACT1* pre-mRNA, despite different pre-mRNAs exhibiting different propensities for cleavage at aberrant sites even in the absence of Prp16. Furthermore, primer extension revealed different preferential cleavage sites for *RPS6A* and *RPL23A* (Supplementary Figure S1C).

Selection of the 5′SS is directed by the 5Ex sequence near the splice site

We speculated that variances in splice site selection among *RPS6A*, *RPL23A* and *ACT1* pre-mRNAs could be attributed to differences in the exon sequence near the 5′SS. To investigate if sequence alterations would impact splice site selection,

we created two *ACT1* variants: V1, in which we changed U to G at the –4 position; and V2, in which we changed AG to GU at the –6 and –7 positions of the 5Ex of the ACAC and G5A-ACAC pre-mRNAs (Figure 2A). We observed that these modifications of the 5Ex sequence had no significant impact on the splicing of the pre-mRNA with a wild-type 5′SS (Supplementary Figure S2). In contrast, splicing of the G5A mutants was considerably affected by these sequence alterations, as demonstrated by the spliceosomes isolated through precipitation with the anti-Ntc20 antibody (Figure 2B). The V2 variant behaved similarly to the original sequence (V0), generating only small amounts of aberrant 5Ex in the absence of Prp16 (Figure 2B, lanes 2 and 6). However, Prp16 promoted aberrant cleavage, particularly for V2 (Figure 2B, lane 5) compared with V0 (Figure 2B, lane 1). V1 exhibited poor splicing efficiency, forming significantly fewer activated spliceosomes than either V0 or V2, and it also generated a higher ratio of aberrant 5Ex in the absence of Prp16 (Figure 2B, lane 4). Similarly, the presence of Prp16 increased the ratio of aberrant to normal 5Ex (Figure 2B, lane 3). These results demonstrate that Prp16 facilitates aberrant cleavage of all three variants of the G5A pre-mRNA. Primer extension analysis of the purified lariat IVS–exon 2 revealed distinct aberrant cleavage sites for each variant (Figure 2C). The primary cleavage sites were at U_{-5} for V0 (Figure 2C, lanes 7 and 8), U_{-4} for V1 (Figure 2C, lanes 2 and 3) and A_{-6} for V2 (Figure 2C, lanes 5 and 6). Additional minor cleavage sites at G_{-8} (Figure 2C, lane 3), A_{-10} (Figure 2C, lanes 5 and 6) and U_{+6} (Figure 2C, lanes 3, 6 and 7) were also detected. These results parallel those observed for *RPL23A* and *RPS6A* (Supplementary Figure S1), indicating that cleavage site selection is influenced by the 5Ex sequence near the 5′SS.

Prp16 promotes branching of G5A pre-mRNA by promoting aberrant 5′ splice site usage

Although Prp16 is not essential for branching of wild-type pre-mRNA, it facilitates the reaction of BP-mutated pre-mRNAs in an ATP-independent manner (17). Our discovery that Prp16 also promotes aberrant 5′SS cleavage of G5A pre-mRNA, independently of ATP (Figure 1), implies a potential common mechanism for Prp16-mediated BP selection and 5′SS selection for pre-mRNAs carrying splice site mutations. The ATPase function of Prp16 is required after the branching step to drive the splicing pathway by remodeling the spliceosome to enable positioning of the 3′SS at the catalytic center. The ATP-independent function of Prp16 is required for the branching reaction when the interaction between the BP and the 5′SS is hindered by mutations, conceivably by stabilizing their interaction to promote the reaction. Our previous study has revealed that the G5A mutation results in abnormal interactions of U5 and U6 with the pre-mRNA at the catalytic center (26), blocking formation of the B^{act} complex by >95% (Supplementary Figure S3). However, a residual level of splicing activity remains detectable in the absence of Prp16. We speculated that while the majority of the G5A spliceosome remains inactive with a distorted RNA catalytic core, a small proportion may still adopt an active conformation. This scenario could explain the observation of leak-through splicing activity where cleavage occurs at the authentic 5′SS and subsequently proceeds to exon ligation. Despite misalignment of the 5′SS and the BP on the misconfigured spliceosome, these elements may interact dynamically and non-specifically. In the presence of Prp16, such interactions are probably stabilized, thereby facilitating the branching reaction, which may progress slowly and imprecisely.

We then conducted a comparative analysis of splicing kinetics of G5A pre-mRNA in the presence or absence of Prp16, measuring branching reaction efficiency and aberrant splice site selection on activated spliceosomes (Figure 3). To prevent progression to the second catalytic reaction, the pre-mRNA also harbored mutations at the 3′SS (ACAC). Activated spliceosomes were isolated by precipitating the splicing reaction using anti-Ntc20 antibody (Figure 3A). In the absence of Prp16, the branching reaction almost plateaued by 30 min with only minimal production of aberrant 5Ex (Figure 3A, lanes 1–4). In the presence of Prp16, more spliceosomes were precipitated by anti-Ntc20 antibody over the same time frame, indicating that Prp16 promotes the formation of active spliceosomes. Furthermore, as the incubation time increased, we observed greater accumulation of spliced products with aberrant 5Ex rather than authentic 5Ex (Figure 3A, lanes 5–8), indicating that the branching reaction was facilitated by Prp16 at the cost of accuracy. To quantify these observations, we calculated the percentage of branching (relative molar amounts of intron–exon 2 over intron–exon 2 plus pre-mRNA) and the percentage of aberrancy (relative molar amounts of aberrant over total 5Ex) over the time course. In the absence of Prp16, both the percentage of branching and aberrancy reached a plateau after 30 min. However, in the presence of Prp16, both measures increased steadily throughout the time course (Figure 3B, C). Together, these results indicate that Prp16 promotes splicing of G5A pre-mRNA by enhancing the efficiency of the branching reaction, although the increase in branching is associated with the erroneous usage of the 5′SS.

G5A mutation disrupts Prp8–pre-mRNA interaction

To understand how Prp16 promotes aberrant 5′SS usage on G5A pre-mRNA, we examined protein–RNA interactions within the 5Ex in the presence or absence of Prp16. We reasoned that Prp16 might enhance the stability of BP interactions with the 5Ex sequence by promoting the binding of proteins that interact with the 5Ex near the splice junction, thereby influencing 5′SS selection. Cryo-electron microscopy (EM) structures of the spliceosome have revealed that the 5Ex is inserted into Prp8 between the linker and N domains, which maintains a consistent structure throughout the splicing pathway after spliceosome activation (18,32–41). Using 4-thiouridine (4sU)-labeled *ACT1* pre-mRNA, we have previously demonstrated cross-linking of Prp8 to positions –2, –9 and –16 of the 5Ex, as well as cross-linking of Cwc24, Prp11 and Yju2 to its –2 position (28). Here, we extended those 4sU cross-linking experiments to examine the effect of Prp16 on interactions of these proteins with the 5Ex of G5A pre-mRNA. To be able to label the pre-mRNA with 4sU at more positions, we introduced three mutations into the 5Ex of *ACT1-ACAC* pre-mRNA (designated as V3), which enabled the incorporation of 4sU at positions –5 and –7 in addition to –2 and –9 (Figure 4A). The V3 pre-mRNA exhibited a slightly lower level of splicing activity than other variants (Supplementary Figure S2).

Splicing reactions performed with ACAC pre-mRNA in the presence of Prp16 were expected to stall the spliceosome prior to exon ligation after release of step-one factors Yju2 and Cwc25, and accumulate the spliceosome C* complex (Figure

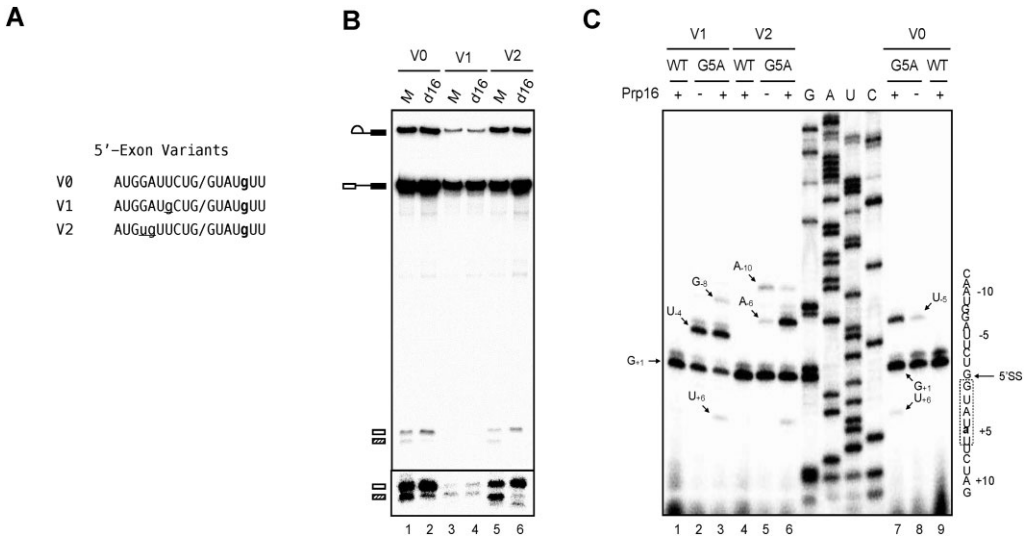

Figure 2. Prp16 promotes aberrant cleavage of the 5′SS at different positions for different 5Ex variants of *ACT1*-G5A pre-mRNA. (**A**) Sequences of the 5Ex variants, V0, V1 and V2, with lower case letters indicating sequence alterations. (**B**) Splicing of ACT1-G5A 5Ex variants was performed using mock-treated (lanes 1, 3 and 5) or Prp16-depleted (lanes 2, 4 and 6) extracts. The reaction mixtures were precipitated with anti-Ntc20 antibody. The lower panel is a longer exposure of the 5Ex region. (**C**) Primer extension using ACT1-A6 primer to map the 5′ cleavage site of wild-type (lanes 1, 4 and 9) or G5A (lanes 2, 3, 5, 6, 7 and 8) 5Ex variant pre-mRNAs in the absence (lanes 2, 5 and 8) or presence (lanes 1, 3, 4, 6, 7 and 9) of Prp16. The consensus 5′SS sequence is boxed.

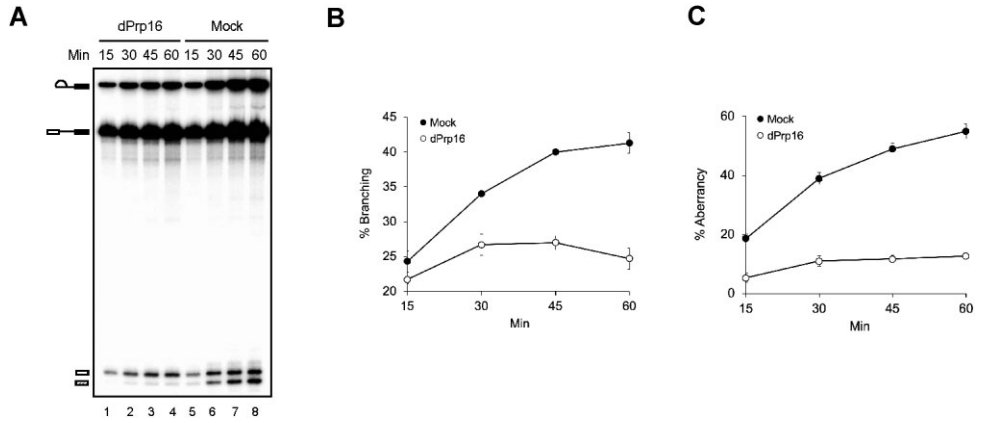

Figure 3. Kinetics of Prp16-facilitated aberrant 5′SS cleavage of ACT1-G5A pre-mRNA. (**A**) Splicing of ACT1-G5A pre-mRNA was performed in Prp16-depleted (lanes 1–4) or mock-treated (lanes 5–8) extracts, and the reaction mixtures were precipitated with anti-Ntc20 antibody. (**B**) Branching efficiency, as measured according to the molar ratio of lariat IVS–exon 2 over lariat IVS–exon 2 plus pre-mRNA. Data represent mean values from three experiments, and standard deviations (SDs) are indicated. (**C**) Percentage of aberrant cleavage, as measured according to the molar ratio of aberrant over total 5Ex. Data represent mean values from three experiments, and SDs are indicated.

4B). Using the V3 pre-mRNA, we observed strong cross-linking of Prp8 to positions –2, –5 and –7; Yju2 exhibited cross-linking to positions –2 and –5; Cwc24 to the –5 position; and Isy1 (also known as Ntc30) to the –2 position (Figure 4C; Supplementary Figure S3). The identities of the cross-linked proteins were confirmed by immunoprecipitation for each specific protein using polyclonal antibodies or monoclonal antibodies against the tags, following treatment of the reaction mixtures with denaturants (Supplementary Figure S4). In the absence of Prp16, the reaction arrested after branching, resulting in complex C accumulation. Under this condition, cross-linking patterns were similar to our Mock control, although cross-linking of Prp8 to the –2 position was weaker (Figure 4D). Both Yju2 and Cwc25 can cross-link to the pre-mRNA when complex C accumulates (19,28,42). The observation of a similar amount of Yju2 cross-linking in the presence of Prp16 implies that Yju2 dynamically re-associates with the stalled spliceosome, as demonstrated previously (20). Cwc24 is required for Prp2-mediated remodeling of the spliceosome for catalytic activation, and is released from the spliceosome together with the SF3a/b and RES (REtention and Splicing) complexes. Cwc24 accumulates on the spliceosome when Prp2 is non-functional (26). We observed strong cross-linking of Cwc24 to the –5 position when splicing reactions were performed in *prp2-1* mutant extracts (Figure 4E; Supplementary Figure S4), but small amounts of –5 cross-linking were also detected in mock-treated (Figure 4C) or Prp16-depleted (Figure 4D) extracts, indicating that some spliceosome remained as the B^{act} complex in these reactions. Thus, the splicing pathway does not appear to be completely synchronized when it is blocked at specific steps, resulting in a variety of complexes. Notably, the intensity of

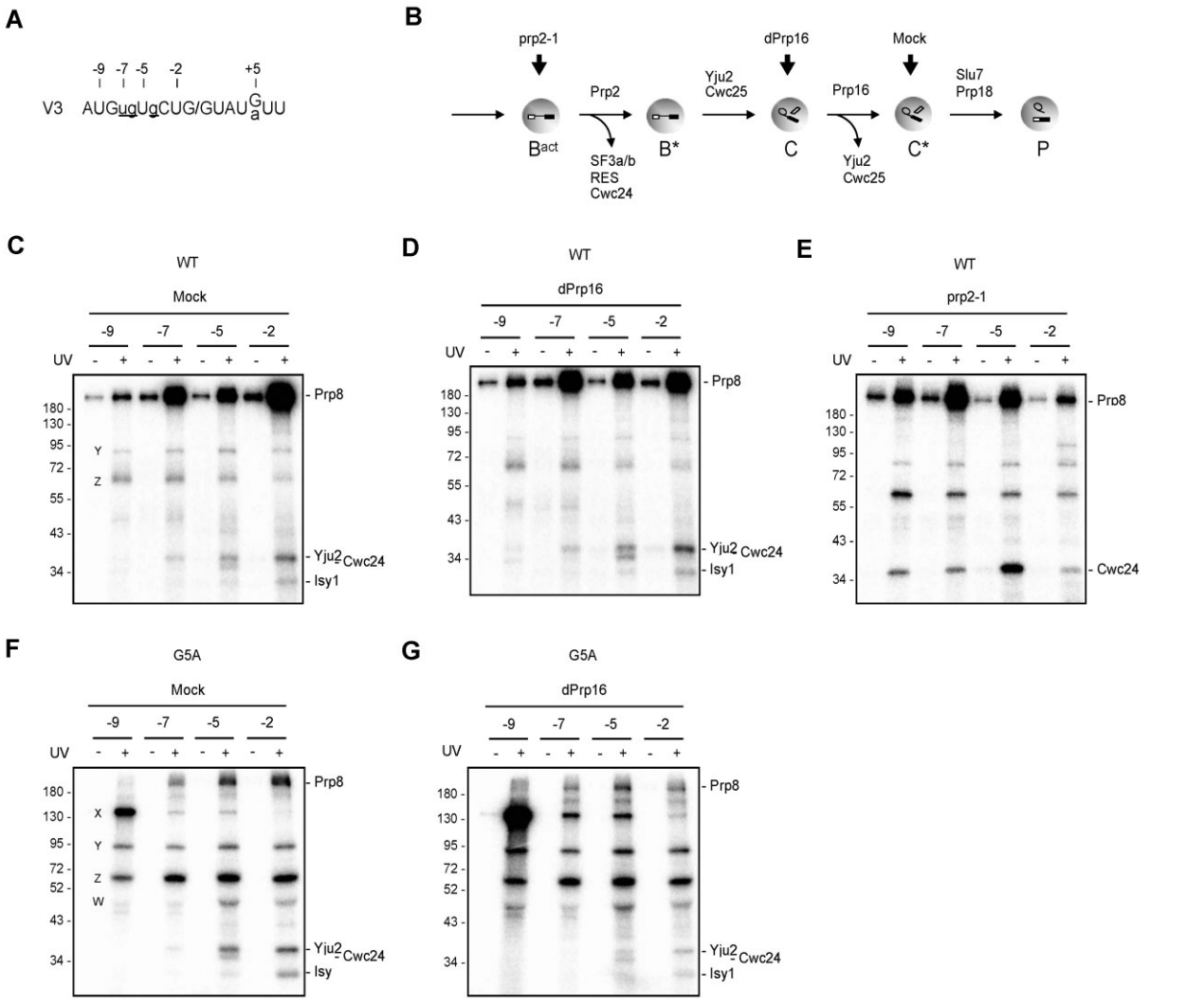

Figure 4. Cross-linking of proteins to the 5Ex by 4sU labeling reveals destabilized interactions between Prp8 and the 5Ex. (**A**) Sequence of the ACT1-G5A-V3 variant, with the 4sU label positions indicated. (**B**) The splicing pathway of post-activated spliceosomes. B^{act}, C or C* complexes accumulate when splicing is performed in the prp2-1 extract, Prp16-depleted extract or using ACAC pre-mRNA, respectively. (**C**–**G**) Crosslinking of proteins to the pre-mRNAs labeled with 4sU at position –2, –5, –7 or –9 in the splicing reactions using wild-type (**C**, **D** and **E**) or G5A mutant (**F** and **G**) ACAC pre-mRNA in mock-treated (C and F), Prp16-depleted (D and G) or prp2-1 extracts, followed by immunoprecipitation of the reaction mixtures with anti-Ntc20 antibody.

Prp8 cross-linking at the –2 position increased as the pathway progressed from complex B^{act} (*prp2-1*) to C (dPrp16) to C* (Mock), whereas relative cross-linking intensities at the –5 and –7 positions remained largely unchanged. This outcome indicates that though Prp8 interacts with the 5Ex over a region spanning at least the –2 to –9 positions after spliceosome activation, it exhibits a more stable interaction with the –2 residue after the branching reaction in preparation for exon ligation.

Since G5A pre-mRNA is severely impaired for formation of the active spliceosome, a much larger volume of splicing reaction was required for our cross-linking analysis relative to the wild-type pre-mRNA, which prompted a significant increase in binding of non-specific proteins (X, Y, Z and W) to immunoprecipitated beads (Figure 4F, G). In this analysis, we observed that cross-linking of Yju2, Cwc24 or Isy1 was either unaffected or only moderately affected by the G5A mutation, whereas cross-linking of Prp8 was substantially weakened (Figure 4F, G), indicating that the G5A mutation primarily impacts the interaction of Prp8 with the 5Ex. Similar to our findings for wild-type pre-mRNA, Prp8 cross-linking at the –2 position was also enhanced for Mock control relative to dPrp16-depleted extracts. Furthermore, Prp8 cross-linking at the –2 and –7 positions was more severely affected compared with the –5 position. In contrast to wild-type pre-mRNA, cross-linking to G5A pre-mRNA at the –2 position was weaker than that at the –5 position in Prp16-depleted extracts (Figure 4F). In mock-treated extracts, cross-linking at the –2 position was slightly stronger than at the –5 position for the G5A pre-mRNA (Figure 4F), but not to the same level as for wild-type pre-mRNA (Figure 4C). We also observed that the relative cross-linking signal intensity at the –2 to –5 position (–2/–5) for G5A in mock-treated extracts (Figure 4F) was more similar to that of wild-type pre-mRNA in Prp16-depleted extracts (Figure 4D), whereas the –2/–5 signal for G5A in Prp16-depleted extracts (Figure 4G) was more similar to wild-type pre-mRNA in *prp2-1* extracts (Figure 4E). Together, these results indicate that splicing of G5A pre-mRNA

proceeds at a slow rate relative to the wild-type pre-mRNA, leading to the stalling of the spliceosomes at even earlier stages when subjected to the same conditions. Nevertheless, the presence of Prp16 facilitates the progression of the splicing pathway.

Prp16 promotes selection of alternative BS on d-brA mutant pre-mRNA by destabilizing Cwc25 from binding to the BS

Prp16 has been implicated in promoting the selection of an alternative BS in an ATP-dependent manner during splicing of BP-modified *UBC4* pre-mRNA, in which the BP adenosine residue was changed to 2′-deoxyadenosine (d-brA) (25). Thus, Prp16 appears to exert seemingly contradictory functions, acting as both a proofreader for the BS and a facilitator for alternative BS selection. Although the ability of Prp16 to promote alternative BS selection aligns with its role in promoting aberrant 5′SS cleavage, the former requires ATP and the latter does not. To gain further insights, we investigated if the function of Prp16 in promoting alternative BS selection is mediated through Cwc25.

Previous studies have demonstrated that Cwc25 is required for the branching reaction, and that it interacts with the spliceosome immediately prior to the reaction (19). Cwc25 transiently associates with the pre-catalytic spliceosome and undergoes tight binding upon branch formation (17). We hypothesized that during the splicing reaction, the d-brA pre-mRNA could form a non-covalent RNA structure resembling a branch that could be recognized by Cwc25. The removal of Cwc25, facilitated by the ATPase activity of Prp16, allows U2 to slide away and explore secondary BS. To investigate this possibility, we used *ACT1* pre-mRNA with brA and d-brA as the BP, and immunoprecipitated activated spliceosomes with anti-Ntc20 antibody to enrich for the complexes (Figure 5). Consistent with previous findings on *UBC4* pre-mRNA, splicing of *ACT1* d-brA pre-mRNA was inhibited in the absence of Prp16 or in the presence of mutant Prp16 (Figure 5A, lanes 9–12), whereas residual activity was detected in the presence of wild-type Prp16 (Figure 5A, lanes 7 and 8). To map the BP sites, we performed primer extension analysis using a primer located downstream of the BP for the reverse transcription reaction, which stops one nucleotide before the BP. We identified two major BP sites at A_{-1} and A_{-14}, along with several minor sites primarily upstream of the BS (Figure 5B). Utilization of A_{-1} as the BP implies a shift of the U2 snRNA Ψ_{35}–A_{-1} base pairing to A_0, causing A_{-1} to bulge out for the branching reaction, which would also require the ATPase activity of Prp16. The secondary preference for BP A_{-14} reflects a putative BP of a CBS, in which the first six nucleotides are identical to the canonical BS and they can form five continuous base pairings with the U2 snRNA. To examine if Cwc25 is associated with the spliceosome only when Prp16 is non-functional, we performed splicing using V5-tagged Cwc25 extracts and precipitated the Cwc25-associated spliceosome with anti-V5 antibody (Figure 5C). For normal substrate (brA), we found that Cwc25 was only detected in association with spliceosomes containing intron–exon 2, or complex C, but not with the pre-mRNA (Figure 5C, lanes 3, 6 and 9). In the case of d-brA, the association of Cwc25 with the pre-mRNA was greatest in the presence of mutant Prp16 (Figure 5C, lane 18), lower in the absence of Prp16 (Figure 5C, lane 15) and least with wild-type Prp16 (Figure 5C, lane 12). These observations are supported by data quantification (Figure 5D). Our results confirm that Cwc25 exhibits stable binding to the branch site of the d-brA spliceosome in the absence of Prp16, and it is even more pronounced in the presence of mutant Prp16, supporting the notion that the ATPase activity of Prp16 promotes Cwc25 release, enabling U2 to dissociate and search for an alternative BS.

Prp16 promotes usage of a mutated branchpoint

Pre-mRNAs with a mutated BP exhibit poor splicing efficiency, resulting in limited product formation. Depletion of Prp16 from the extract impedes even this residual activity (17), indicating that Prp16 facilitates splicing of BP-mutated pre-mRNA. However, it remains unclear if mutated BPs are utilized for branching. To determine which BP is used, we isolated lariat intron–exon 2 from splicing reactions using brC and brG pre-mRNAs for primer extension. Our results reveal that the branching reaction occurred at the same position whether mutated C or G was used, respectively, for branch formation (Figure 6A). Despite minimal production during splicing with the brC or brG pre-mRNA in the absence of Prp16, we enriched for spliceosomes by immunoprecipitation and isolated intron–exon 2 for primer extension analysis. We detected that branching of both the brC and brG mutants occurred at two sites: one at the authentic site utilizing the mutated BP, C/G, and the other at the CBS (Figure 6B, lanes 1 and 4). Although branching efficiency was comparable at both sites for the brC pre-mRNA (Figure 6B, lane 1), brG exhibited reduced branching at the CBS (Figure 6B, lane 4). This outcome indicates that in the absence of Prp16, U2 may dissociate from the authentic BS to explore alternative secondary BSs when the BP is mutated. Prp16 promotes the reaction at the authentic BS, potentially by enhancing the stability of the interaction between the BP and the 5′SS, thereby preventing U2 from moving away.

Discussion

New insights into splicing fidelity control by Prp16

Prp16 was originally identified as a suppressor of the brC mutation of pre-mRNAs, enabling splicing when the ATPase activity of Prp16 was compromised. Subsequent studies have revealed that Prp16 is required for the splicing reaction only after lariat formation (16,21). Further investigations have illuminated a correlation between Prp16's ATPase activity and the strength of suppression, giving rise to a hypothesis of a proofreading mechanism governing splicing fidelity control regulated by Prp16. According to the proposed model (Figure 7A), following branching, the spliceosome undergoes a conformational change before ATP hydrolysis catalyzed by Prp16. The conformational change step is crucial as it marks the commitment of the spliceosome to productive splicing. Mutation at the BP hinders this conformational transition, affording Prp16 more time for ATP hydrolysis before the conformational alteration takes place. This results in formation of a defective spliceosome that cannot progress through the splicing pathway. Reducing Prp16's ATPase activity allows more time for the conformational shift to take place, thereby facilitating pathway progression and ultimately supporting cell survival (22). Nevertheless, the postulated conformational change has never been directly demonstrated.

Prp16's role in proofreading was further extended to the 5′SS. This activity was demonstrated in an experiment show-

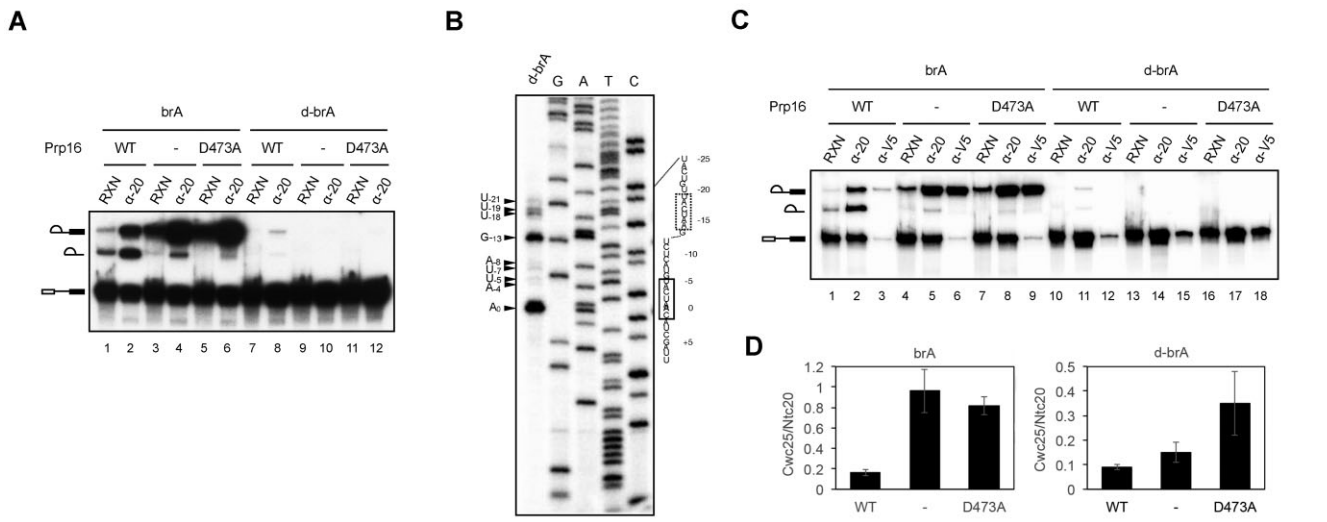

Figure 5. Prp16 promotes release of Cwc25 from d-brA pre-mRNA, thereby allowing U2 to search for alternative branch sites. (**A**) Splicing of brA or d-brA pre-mRNA was performed in Prp16-depleted extracts without (lanes 3, 4, 9 and 10) or supplemented with wild-type Prp16 (lanes 1, 2, 7 and 8) or the D473A mutant (lanes 5, 6, 11 and 12), before precipitating the reaction mixtures with anti-Ntc20 antibodies (lanes 2, 4, 6, 8, 10 and 12). RXN, 1/10 of reaction mix. (**B**) Primer extension of lariat IVS–exon 2 isolated from the immunoprecipitate of the d-brA reaction using primer ACT1-A7 to map the BP. The BS is surrounded by a solid line and the CBS is surrounded by a dotted line. (**C**) Splicing of brA or d-brA pre-mRNA was performed in Prp16-depleted Cwc25-V5 extracts without (lanes 4–6 and 13–15) or supplemented with wild-type Prp16 (lanes 1–3 and 10–12) or the D473A mutant (lanes 7–9 and 16–18), before precipitating the reaction mixtures with anti-Ntc20 (lanes 2, 5, 8, 11, 14 and 17) or anti-V5 (lanes 3, 6, 9, 12, 15 and 18) antibody. RXN, 1/10 of reaction mix. (**D**) Quantification of the proportion of Cwc25-associated spliceosomes over activated spliceosomes assembled on brA or d-brA pre-mRNA. Data represent mean values from three experiments, and SDs are indicated.

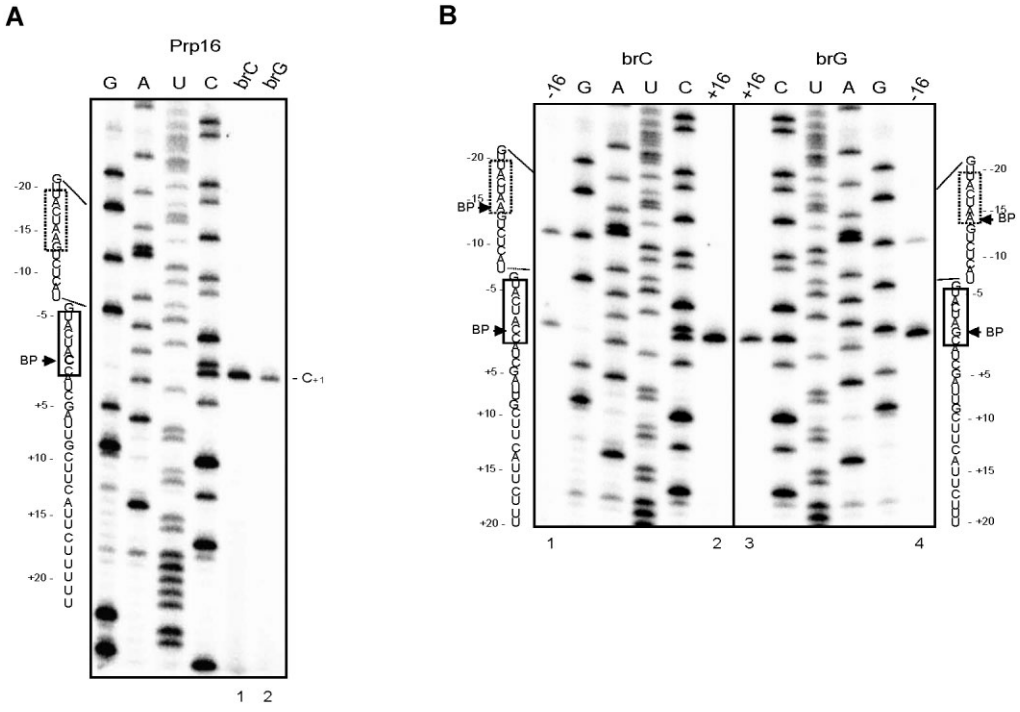

Figure 6. Prp16 prevents usage of the CBS for brC and brG mutant pre-mRNAs. Primer extension of lariat IVS–exon 2 isolated from the spliceosome assembled on brC or brG pre-mRNAs in the presence (**A**, lanes 1 and 2; **B**, lanes 2 and 3) or absence (**B**, lanes 1 and 4) of Prp16 using primer ACT1-A7.

ing that splicing was inhibited prior to 5′SS cleavage when a non-bridging oxygen at position U80 of U6 snRNA was replaced with sulfur. Subsequent incubation of the purified spliceosome with Mg^{2+} revealed that 5′SS cleavage occurs only in the absence of ATP or using the ATPase mutants of Prp16 (24). It was proposed that, like the BP mutant, Prp16 drives the removal of the stalled spliceosome by catalyzing ATP hydrolysis. Unlike the case proposed for the BP mutant, Prp16 acts before the branching reaction but, in both scenarios, Prp43 plays a role in discarding the stalled spliceosomes (24,43).

Previously, we have demonstrated that Prp16 normally functions after branching to facilitate release of the key step-

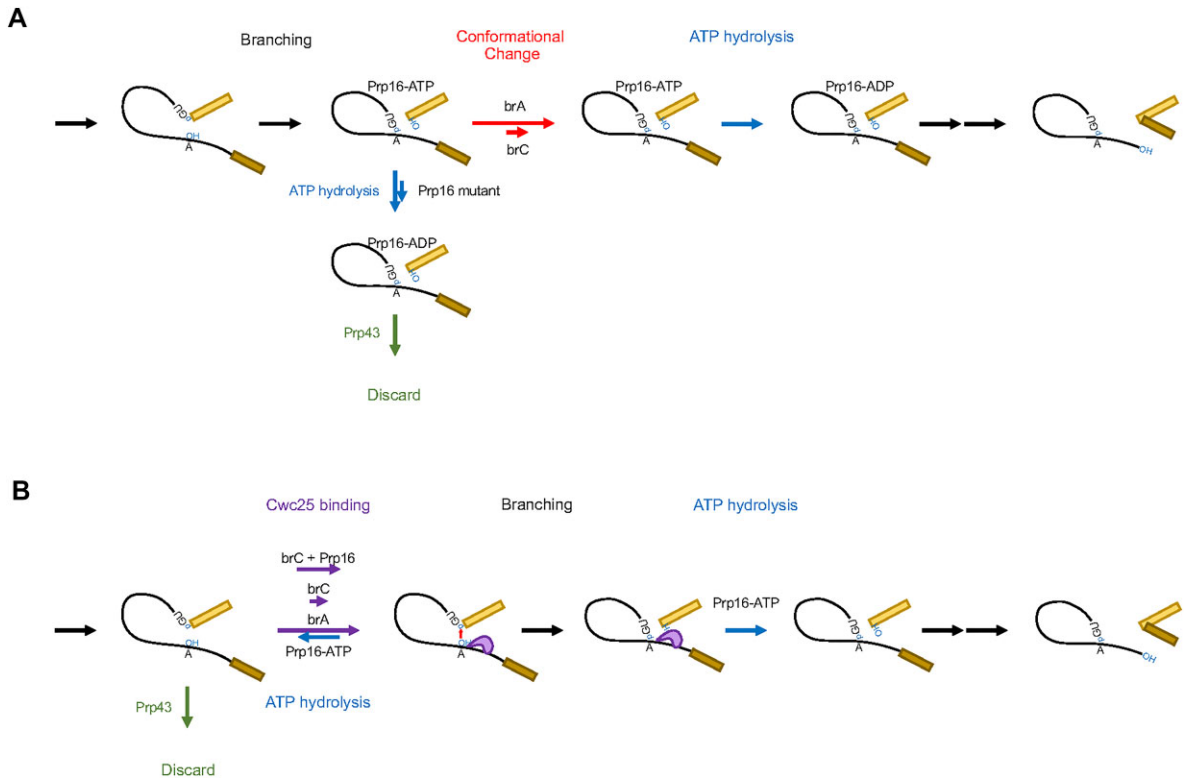

Figure 7. Comparison between two kinetic proofreading mechanisms for Prp16-mediated proofreading of brC pre-mRNA. (**A**) A previous hypothesis proposed that following branch formation, Prp16 is associated with the spliceosome. Before Prp16 catalyzes ATP hydrolysis, the spliceosome must undergo a conformational change for its commitment to productive splicing. For brC mutant pre-mRNA, the conformational change is hindered, leading to ATP hydrolysis occurring before the conformational alteration, thereby forming a defective spliceosome, which can be eliminated through the action of Prp43. The ATPase mutants of Prp16 allow more time for the conformational shift to take place. (**B**) Our current model suggests that Cwc25 binds to the spliceosome upon catalytic activation of the spliceosome, a state vulnerable to Prp43-mediated spliceosome disassembly. The branching reaction occurs immediately upon Cwc25 binding. Cwc25 is subsequently released from the spliceosome, mediated by Prp16-catalyzed ATP hydrolysis, to allow for the positioning of the 3′SS. With brC mutation, the association of Cwc25 with the spliceosome is weak, permitting easy dissociation via ATP hydrolysis. This function serves to proofread the BS. However, Prp16 also enhances the stability of Cwc25 to promote branching in the absence of ATP hydrolysis. The purple object represents Cwc25.

one factor Cwc25. Cwc25 binds to the spliceosome upon catalytic activation of the spliceosome (formation of the B* complex), and the branching reaction occurs immediately upon its binding. Cwc25 exhibits weak binding affinity for the B* complex, but becomes strongly bound after branching upon formation of the spliceosome C complex (17). Cwc25, along with Yju2 and Isy1, is located in the spliceosome's catalytic center as revealed by cryo-EM structures of the spliceosome C complex (18,32). In order for exon ligation to occur, Prp16-catalyzed ATP hydrolysis is necessary to displace Cwc25 and Yju2 from the catalytic center to allow positioning of the 3′SS (17). However, Prp16 also enhances binding of Cwc25 to the spliceosome to promote the branching reaction, independently of ATP, but this function is only noticeable during splicing of suboptimal substrates when splicing proceeds at slow rates (17) (Figure 7B). Cryo-EM structures of the spliceosome C complex have revealed that a long α-helix of Cwc25 spanning amino acid residues 2–16 inserts into the active site, interacting with the bulged branch helix (18,32). When the BP is mutated, the branching reaction is impaired due to weak Cwc25 interaction. A cryo-EM structure of the spliceosome Ci complex, an intermediate complex in the transition from the C to C* spliceosome, has revealed interactions between Prp16, Cwc25 and Yju2 (44), indicating that Prp16 may stabilize the Cwc25 binding by directly interacting with the protein.

The interplay between the ATP-dependent and ATP-independent functions of Prp16 governs the efficiency of the splicing reaction in that one function destabilizes Cwc25 to prevent branching, and the other stabilizes Cwc25 binding to promote branching. Prp16 mutants with reduced ATPase activity prolong retention of Cwc25 on the pre-catalytic spliceosome, resulting in increased splicing activity. Differing from the initial proofreading model, which implies that Prp16 directs the defective spliceosome to a discard pathway after branching, we suggest that Prp16 plays a role in proofreading the BP by removing Cwc25 prior to the branching reaction, allowing the spliceosome to revert to the state of the B* complex, which can either re-enter the splicing pathway or be subjected to disassembly. A comparison of our and previous models is presented in Figure 7.

We have demonstrated previously that during the catalytic reactions, spliceosomes stalled in the middle of the pathway are susceptible to Prp43-mediated spliceosome disassembly at defined stages; specifically, after the action of the DExD/H-box RNA helicases, Prp2 and Prp16. Both proteins play roles in facilitating the release of components binding at the catalytic center—SF3a/b for Prp2, and Cwc25 and Yju2 for

Prp16—in preparation for a structural alteration at the catalytic center (45). The B* complex forms after the action of Prp2, and is vulnerable to Prp43-mediated disassembly. Therefore, Prp16 functions as a checkpoint by removing Cwc25 from the spliceosome prior to branching when the reaction is hindered, rendering the spliceosome vulnerable to disassembly. This interpretation is in line with the fundamental concept of Prp16's role in proofreading through ATP hydrolysis. Nevertheless, it differs in that proofreading operates prior to branching instead of following it. Additionally, the elimination mechanism takes place in a linear pathway, as opposed to diverting it towards a branched pathway postulated in a previous model (22,23) (Figure 7). Notably, a similar mechanism has been proposed for Prp22 in proofreading the 3′SS by rejecting the stalled spliceosome prior to the exon ligation reaction and discarding the spliceosome in a linear pathway (30).

The revelation of the ATP-independent activity of Prp16 in promoting branching of suboptimal substrates complicates the rationale for Prp16's role in ensuring splicing fidelity. Prp16 can prevent branching by eliminating Cwc25, yet can also promote branching by enhancing the stability of Cwc25. This paradoxical functionality casts doubts on the active involvement of Prp16 in proofreading splice sites. It is worth noting that the model was initially put forth to provide an explanation for the observed suppression of brC mutation by *PRP16* ATPase mutants. Conversely, it suggests that Prp16's primary function is to propel the splicing process forward. The ATPase activity of Prp16 functions after branching to aid in the liberation of Cwc25, thereby enabling exon ligation. The ATP-independent activity of Prp16 serves to facilitate the branching reaction when the reaction is impeded due to mutations at the BP.

Cwc25 stabilizes the U2–BS interaction on the pre-catalytic spliceosome

In the absence of Prp16, both the authentic and cryptic BSs were utilized for splicing of brC and brG pre-mRNAs, albeit with extremely low efficiency. In the presence of Prp16, the splicing efficiency increased, but only the authentic site was used. This observation reveals the dynamic nature of the interaction between U2 and the BS prior to branching, and indicates that the ATP-independent function of Prp16, which restrains Cwc25, plays a crucial role in stabilizing the U2–BS interaction before the branching reaction occurs. This stabilization prevents U2 from shifting towards the CBS. Notably, the proportion of branching events occurring at the cryptic site relative to the authentic site was higher for brC compared with brG pre-mRNAs. This discrepancy indicates that the branching efficiency at the BS-brC was lower due to a greater steric constraint caused by the transversion mutation at the BP, thereby allowing U2 to dissociate more easily.

In this study, we have also elucidated the mechanism underlying Prp16's requirement for ATPase activity to select alternative BSs in d-brA pre-mRNA. We show that Prp16 promotes alternative BS selection through its influence on Cwc25. Although the BP of d-brA pre-mRNA is unreactive, it does not impact the overall structure of the BS–U2, BS–5′SS or RNA–protein interactions at the catalytic center. It is likely that a non-covalent branch-like structure forms, which stabilizes Cwc25 binding. Upon ATP hydrolysis, Prp16 disrupts that binding of Cwc25, whereas the ATPase mutant of Prp16 stabilizes it, resulting in either reduced or increased retention of Cwc25 on the spliceosome, respectively, and consequently allowing U2 to scan along the pre-mRNA to search for an alternative BS. Interestingly, when the authentic BP is not reactive, multiple BPs on the *ACT1* intron could be used, but all were located upstream. This result suggests that when the U2–BS interaction is destabilized in the absence of Cwc25, U2 may undergo unidirectional translocation in the 3′ to 5′ polarity to search for alternative BS sequences. We have recently demonstrated the highly dynamic nature of U2–BS interactions during formation of the pre-spliceosome, and that U2 also translocates in a 3′ to 5′ direction to search for the BS upon loading onto the pre-mRNA (46). The factors that restrict this unidirectional translocation of U2 during both stages of the splicing pathway remain unclear. Our findings shed light on the intricate process of alternative BS selection and provide insights into the dynamic nature of U2–BS interactions in the absence of Cwc25.

Prp16 promotes branching of 5′SS-mutated pre-mRNAs

The catalytic center of the spliceosome is orchestrated by base pairings between the 5′SS, U6 and U2, with RNA–RNA interactions being stabilized by the binding of protein components. Upon spliceosome activation, the 5Ex is integrated into Prp8, enclosed by the linker and N domains (47). This part of the structure remains unchanged in the subsequent steps of the splicing reaction (18,32–41). The G5A mutation severely impacted the cross-linking ability of Prp8 with all positions of the 5Ex we examined, but it did not grossly affect cross-linking of Yju2, Cwc24 or Isy1 as much. It is conceivable that distortion of the RNA catalytic core, caused by the G5A mutation, disturbs the structure of Prp8, leading to weakened interactions between Prp8 and the 5Ex. Being no longer restrained by Prp8, the 5Ex may move along the Prp8 tunnel, exposing its sequence to the spliceosome's catalytic center, and thereby enabling interaction with the BS. This results in aberrant cleavage at the 5Ex. Since the 5Ex can move dynamically due to weak interactions with Prp8, the reaction only occurs slowly and with lower specificity. This process also requires Cwc25 to stabilize the interaction of the BP with the 5Ex, with interaction between Prp16 and Cwc25 further enhancing BP–5Ex stability.

The ATP-independent function of Prp16 has previously been implicated as also acting on the 5′SS based on the observation that Prp16 could promote the branching reaction independently of its ATPase activity when splicing was impeded by substituting a non-bridging oxygen of U6–U80 with sulfur (24). However, the precise mechanism by which Prp16 acts on the 5′SS had been unclear. In this study, we demonstrate that this function of Prp16 also facilitates branching of pre-mRNA harboring a G5A mutation or when the 5′SS-binding protein Cwc24 is depleted from extracts. We have previously elucidated how Prp16 promotes branching of the BS-mutated pre-mRNA through its action on Cwc25 (17), but whether a similar mechanism applied to the 5′SS was unknown. Prp16 is detectable in cryo-EM structures of the spliceosome C, Ci and C* complexes, but it is only present at the periphery of these structures, with its N-terminal domain being invisible (18,32,34,44). Two-hybrid assays have revealed that Prp16 interacts with Brr2 (48), which is also located at the periphery of the spliceosome. A previous cross-linking analysis using 4sU-

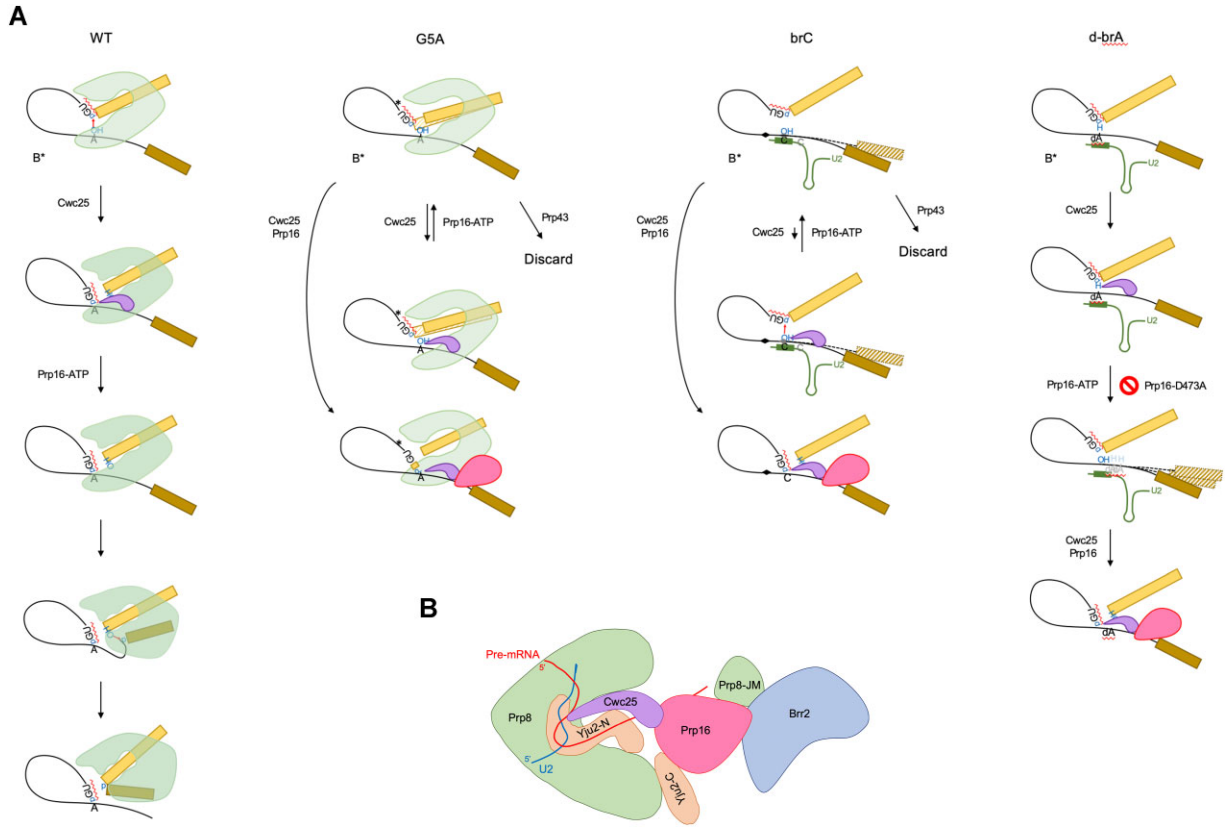

Figure 8. A model for how Prp16 promotes branching of suboptimal substrates by acting through Cwc25. (**A**) Mechanisms of splicing pathways for various modified pre-mRNAs. After catalytic activation of the spliceosome, Cwc25 is recruited to the spliceosome B* complex. The B* complex is accessible to Prp43 and its cofactors, which could disassemble it if stalled for an extended period. For wild-type pre-mRNA, the branching reaction occurs immediately upon the binding of Cwc25, which then firmly associates with the spliceosome, with its N-terminal region contacting the BP. Prp16 facilitates the release of Cwc25 by hydrolyzing ATP, enabling the positioning of the 3′SS to the catalytic center for exon ligation. For G5A pre-mRNA, Prp8 loosely and dynamically interacts with the 5Ex. The branching reaction proceeds very slowly, and Cwc25 is easily released upon Prp16-catalyzed ATP hydrolysis before branching can occur. If the spliceosome remains at the B* state for an extended duration, it is more prone to Prp43-mediated disassembly, akin to a discard pathway. Without ATP hydrolysis, Prp16 stabilizes the binding of Cwc25, thereby promoting the branching reaction. Prp16 interacts with the intron downstream of the Cwc25-interacting site and facilitates the release of Cwc25 upon ATP hydrolysis. For brC pre-mRNA, Cwc25 displays weak affinity for the spliceosome, and the branching reaction also proceeds slowly. As with G5A pre-mRNA, Cwc25 is easily dissociated from the spliceosome through ATP hydrolysis, and is stabilized by the binding of Prp16 without ATP hydrolysis. The release of Cwc25 makes the spliceosome susceptible to Prp43-mediated disassembly. Moreover, weak interaction of Cwc25 leads to less stable U2–BS interaction, allowing U2 to dissociate from the BS to search for alternative BS sites. For d-brA pre-mRNA, catalytic activation and binding of Cwc25 lead to formation of a non-covalent lariat-like structure. Prp16 mediates the release of Cwc25 by hydrolyzing ATP, resulting in a weaker U2–BS interaction and allowing U2 to dissociate and search for an alternative BS. The binding of Cwc25 and Prp16 promotes branching at these alternative sites. The D473A mutant of Prp16 prevents the release of Cwc25 and further enhances its stability on the spliceosome, consequently inhibiting the branching reaction. Prp8 (shown for the N and linker domains), Cwc25 and Prp16 are depicted as green, purple and red objects, respectively. U2 is shown in green, with its BS-interacting region depicted as a green box. The hatched exons and dotted introns represent dynamic interaction of these regions of the pre-mRNA with the spliceosome. (**B**) A diagram illustrating the arrangement of Cwc25 and Yju2 within the catalytic center of the spliceosome, and their interactions with Prp16, Prp8 and the pre-mRNA derived from spliceosome C and Ci complexes and cross-linking studies.

modified pre-mRNAs revealed that Prp16 interacts with the pre-mRNA at a site ∼18–25 or 8–18 nucleotides downstream of the BS in the absence or presence of its ATPase function, respectively (28), indicating that Prp16 translocates from its docking site towards the spliceosome core in the 3′ to 5′ polarity during the splicing reaction. Prp16 was also previously observed to interact with the intron ∼18–22 nucleotides downstream of the BS, corresponding to its docking site, as well as with Yju2 and Cwc25 on the Ci complex (44), implying that Prp16 may stabilize Cwc25 binding through direct interaction. It is possible that Prp16 is recruited to the spliceosome through its interaction with Brr2, and then is transferred onto the pre-mRNA at its docking site. Thus, Prp16 may conduct its ATP-independent function either via its interaction with Brr2 or by docking onto the pre-mRNA.

A model for collaborative action of Prp16 and Cwc25 in promoting branching and proofreading splice sites

In summary, we have uncovered an unappreciated role for Prp16 in promoting aberrant splicing at both the 5′SS and the BS, which strongly contrasts with its established role in maintaining splicing fidelity. We have gained insights into how Prp16 facilitates branching by employing an ATP-independent mechanism when splicing is slowed due to mutation at the 5′SS or the BS. We also provide evidence showing Cwc25 as a mediator of Prp16's activities. We present a model elucidating collaborative action of Prp16 and Cwc25 in promoting branching of suboptimal substrates and in proofreading splice site sequences in Figure 8A. The arrangement of Cwc25 and Yju2 at the catalytic center of the spliceosome, and their in-

teractions with Prp16 and the pre-mRNA, are also elucidated in Figure 8B.

Following the catalytic activation of the spliceosome, Cwc25 is recruited to the spliceosome B* complex. In the case of wild-type pre-mRNA, the branching reaction occurs immediately upon the binding of Cwc25, which then firmly associates with the spliceosome. Prp16 facilitates the release of Cwc25 by hydrolyzing ATP, enabling the positioning of the 3′SS to the catalytic center for exon ligation. For G5A pre-mRNA, Prp8 loosely and dynamically interacts with the 5Ex. The branching reaction proceeds very slowly, and Cwc25 is easily released upon Prp16-catalyzed ATP hydrolysis before branching can occur. If the spliceosome remains at the B* state for an extended duration, it is prone to Prp43-mediated disassembly. Without ATP hydrolysis, Prp16 stabilizes the binding of Cwc25, thereby promoting the branching reaction. In the case of brC pre-mRNA, Cwc25 displays weak affinity for the spliceosome, and the branching reaction also proceeds slowly. As for G5A pre-mRNA, Cwc25 is easily dissociated from the spliceosome through ATP hydrolysis, and is stabilized by the binding of Prp16 without ATP hydrolysis. The release of Cwc25 renders the spliceosome susceptible to Prp43-mediated disassembly. Moreover, weak interaction of Cwc25 leads to less stable U2–BS interaction, allowing U2 to dissociate from the BS to search for alternative BSs. In the case of d-brA pre-mRNA, catalytic activation and binding of Cwc25 lead to formation of a non-covalent lariat-like structure. Prp16 mediates the release of Cwc25 by hydrolyzing ATP, resulting in a weaker U2–BS interaction and allowing U2 to dissociate and search for an alternative BS. The binding of Cwc25 and Prp16 promotes branching at these alternative sites. The D473A mutant of Prp16 prevents the release of Cwc25 and further enhances its stability on the spliceosome, consequently inhibiting the branching reaction.

Data availability

The data underlying this article are available in the article and in its online supplementary data.

Supplementary data

Supplementary Data are available at NAR Online.

Acknowledgements

We thank Nan-Ying Wu for technical assistance, members of the Cheng lab for helpful discussions, and John O'Brien for English editing.

Funding

The Ministry of Science and Technology (Taiwan) [MoST 110-2311-B-001-041 and 111-2311-B-001-008-MY3].

Conflict of interest statement

None declared.

References

1. Wahl,M.C., Will,C.L. and Lührmann,R. (2009) The spliceosome: design principles of a dynamic RNP machine. *Cell*, **136**, 701–718.
2. Will,C.L. and Lührmann,R. (2011) Spliceosome structure and funtion. *Cold Spring Harb. Perspect. Biol.*, **3**, a003707.
3. Pikielny,C.W. and Rosbash,M. (1986) Specific small nuclear RNAs are associated with yeast spliceosomes. *Cell*, **45**, 869–877.
4. Bindereif,A. and Green,M.R. (1987) An ordered pathway of snRNP binding during mammalian pre-mRNA splicing complex assembly. *EMBO J.*, **6**, 2415–2424.
5. Cheng,S.-C. and Abelson,J. (1987) Spliceosome assembly in yeast. *Genes Dev.*, **1**, 1014–1027.
6. Konarska,M.M. and Sharp,P.A. (1987) Interactions between small nuclear ribonucleoprotein particles in formation of spliceosomes. *Cell*, **49**, 763–774.
7. Tarn,W.-Y., Lee,K.-R. and Cheng,S.-C. (1993a) The yeast PRP19 protein is not tightly associated with small nuclear RNAs, but appears to associate with the spliceosome after binding of U2 to the pre-mRNA and prior to formation of the functional spliceosome. *Mol. Cell. Biol.*, **13**, 1883–1891.
8. Tarn,W.-Y., Lee,K.-R. and Cheng,S.-C. (1993b) Yeast precursor mRNA processing protein PRP19 associates with the spliceosome concomitant with or just after dissociation of U4 small nuclear RNA. *Proc. Natl Acad. Sci. USA*, **90**, 10821–10825.
9. Tarn,W.-Y., Hsu,C.-H., Huang,K.-T., Chen,H.-R., Kao,H.-Y., Lee,K.-R. and Cheng,S.-C. (1994) Functional association of essential splicing factor(s) with PRP19 in a protein complex. *EMBO J.*, **13**, 2421–2431.
10. Madhani,H.D. and Guthrie,C. (1992) A novel base-pairing interaction between U2 and U6 snRNAs suggests a mechanism for the catalytic activation of the spliceosome. *Cell*, **71**, 803–818.
11. Sawa,H. and Shimura,Y. (1992) Association of U6 snRNA with the 5′-splice site region of pre-mRNA in the spliceosome. *Genes Dev.*, **6**, 244–254.
12. Cordin,O. and Beggs,J.D. (2013) RNA helicases in splicing. *RNA Biol.*, **10**, 83–95.
13. Cordin,O., Hahn,D. and Beggs,J.D. (2012) Structure, function and regulation of spliceosomal RNA helicases. *Curr. Opin. Cell Biol.*, **24**, 431–438.
14. Liu,Y.-C. and Cheng,S.-C. (2015) Functional roles of DExD/H-box RNA helicases in pre-mRNA splicing. *J. Biomed. Sci.*, **22**, 54.
15. Lin,R.-J., Lustig,A.J. and Abelson,J. (1987) Splicing of yeast nuclear pre-mRNA in vitro requires a functional 40S spliceosome and several extrinsic factors. *Genes Dev.*, **1**, 7–18.
16. Schwer,B. and Guthrie,C. (1991) PRP16 is an RNA-dependent ATPase that interacts transiently with the spliceosome. *Nature*, **349**, 494–499.
17. Tseng,C.-K., Liu,H.-L. and Cheng,S.-C. (2011) DEAH-box ATPase Prp16 has dual roles in remodeling of the spliceosome in catalytic steps. *RNA*, **17**, 145–154.
18. Wan,R., Yan,C., Bai,R., Huang,G. and Shi,Y. (2016) Structure of a yeast catalytic step I spliceosome at 3.4 Å resolution. *Science*, **353**, 895–904.
19. Chiu,Y.-F., Liu,Y.-C., Chiang,T.-W., Yeh,T.-C., Tseng,C.-K., Wu,N.-Y. and Cheng,S.-C. (2009) Cwc25 is a novel splicing factor required after Prp2 and Yju2 to facilitate the first catalytic reaction. *Mol. Cell. Biol.*, **29**, 5671–5678.
20. Tseng,C.-K., Chung,C.-S., Chen,H.-C. and Cheng,S.-C. (2017) A central role of Cwc25 in spliceosome dynamics during catalytic phase of pre-mRNA splicing. *RNA*, **23**, 546–556.
21. Burgess,S., Couto,J.R. and Guthrie,C. (1990) A putative ATP binding protein influences the fidelity of branchpoint recognition in yeast splicing. *Cell*, **60**, 705–717.
22. Burgess,S.M. and Guthrie,C. (1993a) A mechanism to enhance mRNA splicing fidelity: the RNA-dependent ATPase Prp16 governs usage of a discard pathway for aberrant lariat intermediates. *Cell*, **73**, 1377–1392.
23. Burgess,S.M. and Guthrie,C. (1993b) Beat the clock: paradigms for NTPases in the maintenance of biological fidelity. *Trends Biochem. Sci.*, **18**, 381–384.

24. Koodathingal,P., Novak,T., Piccirilli,J.A. and Staley,J.P. (2010) The DEAH box ATPases Prp16 and Prp43 cooperate to proofread 5′ splice site cleavage during pre-mRNA splicing. *Mol. Cell*, **39**, 385–395.
25. Semlow,D.R., Blanco,M.R., Walter,N.G. and Staley,J.P. (2016) Spliceosomeal DEAH-box ATPase remodel pre-mRNA to activate alternative splice sites. *Cell*, **164**, 985–998.
26. Wu,N.-Y., Chung,C.-S. and Cheng,S.-C. (2017) Role of Cwc24 in the first catalytic step and fidelity in 5′ splice site selection. *Mol. Cell. Biol.*, **37**, e00580–e00516.
27. Cheng,S.-C., Newman,A., Lin,R.-J., McFarland,G.D. and Abelson,J.N. (1990) Preparation and fractionation of yeast splicing extract. *Methods Enzymol.*, **181**, 89–96.
28. Chung,C.-S., Tseng,C.-K., Lai,Y.-H., Wang,H.-F., Newman,A.J. and Cheng,S.-C. (2019) Dynamic interactions of proteins with pre-mRNA in mediating splicing catalysis. *Nucleic Acids Res.*, **47**, 899–910.
29. Chan,S.-P., Kao,D.-I., Tsai,W.-Y. and Cheng,S.-C. (2003) The Prp19p-associated complex in spliceosome activation. *Science*, **302**, 279–282.
30. Mayas,R.M., Maita,H. and Staley,J.P. (2006) Exon ligation is proofread by the DExD/H-box ATPase Prp22p. *Nat. Struct. Mol. Biol.*, **13**, 482–490.
31. Parker,R. and Guthrie,C. (1985) A point mutation in the conserved hexanucleotide at a yeast 5' splice junction uncouples recognition, cleavage, and ligation. *Cell*, **41**, 107–118.
32. Galej,W.P., Wilkinson,M.E., Fica,S.M., Oubridge,C., Newman,A.J. and Nagai,K. (2016) Cryo-EM structure of the spliceosome immediately after branching. *Nature*, **537**, 197–201.
33. Rauhut,R., Fabrizio,P., Dybkov,O., Hartmuth,K., Pena,V., Chari,A., Kumar,V., Lee,C.-T., Urlaub,H., Kastner,B., *et al.* (2016) Molecular architecture of the *Saccharomyces cerevisiae* activated spliceosome. *Science*, **353**, 1399–1405.
34. Yan,C., Wan,R., Bai,R., Huang,G. and Shi,Y. (2017) Structure of a yeast step II catalytically activated spliceosome. *Science*, **355**, 149–155.
35. Fica,S.M., Oubridge,C., Galej,W.P., Wilkinson,M.E., Bai,X.-C., Newman,A.J. and Nagai,K. (2017) Structure of a spliceosome remodeled for exon ligation. *Nature*, **542**, 377–380.
36. Bertram,K., Agafonov,D.E., Liu,W.-T., Dybkov,O., Will,C.L., Hartmuth,K., Urlaub,H., Kastner,B., Stark,H. and Lührmann,R. (2017) Cryo-EM structure of a human spliceosome activated for step 2 of splicing. *Nature*, **542**, 318–323.
37. Bai,R., Yan,C., Wan,R., Lei,J. and Shi,Y. (2017) Structure of the post-catalytic spliceosome from *Saccharomyces cerevisiae*. *Cell*, **171**, 1589–1598.
38. Liu,S., Li,X., Zhang,L., Jiang,J., Hill,R.C., Cui,Y., Hansen,K.C., Zhou,Z.H. and Zhao,R. (2017) Structure of the yeast spliceosomal postcatalytic P complex. *Science*, **358**, 1278–1283.
39. Wilkinson,M.E., Fica,S.M., Galej,W.P., Norman,C.M., Newman,A.J. and Nagai,K. (2017) Postcatalytic spliceosome structure reveals mechanism of 3′-splice site selection. *Science*, **358**, 1283–1288.
40. Zhang,X., Yan,C., Hang,J., Finci,L.I., Lei,J. and Shi,Y. (2017) An atomic structure of the human spliceosome. *Cell*, **169**, 918–929.
41. Townsend,C., Leelaram,M.N., Agafonov,D.E., Dybkov,O., Will,C.L., Bertram,K., Urlaub,H., Kastner,B., Stark,H. and Lührmann,R. (2021) Mechanism of protein-guided folding of the active site U2/U6 RNA during spliceosome activation. *Science*, **370**, eabc3753.
42. Liu,Y.-C., Chen,H.-C., Wu,N.-Y. and Cheng,S.-C. (2007) A novel splicing factor Yju2 is associated with NTC and acts after Prp2 in promoting the first catalytic reaction of pre-mRNA splicing. *Mol. Cell. Biol.*, **27**, 5403–5413.
43. Mayas,R.M., Maita,H., Semlow,D.R. and Staley,J.P. (2010) Spliceosome discards intermediates via the DEAH box ATPase Prp43p. *Proc. Natl Acad. Sci. USA*, **107**, 10020–10025.
44. Wilkinson,M.E., Fica,S.M., Galej,W.P. and Nagai,K. (2021) Structural basis for conformational equilibrium of the catalytic spliceosome. *Mol. Cell*, **81**, 1439–1452.
45. Chen,H.-C., Tseng,C.-K., Tsai,R.-T., Chung,C.-S. and Cheng,S.-C. (2013) Link of NTR-mediated spliceosome disassembly with DEAH-box ATPases Prp2, Prp16 and Prp22. *Mol. Cell. Biol.*, **33**, 514–525.
46. Kao,C.-Y., Cao,E.-C., Wai,H.L. and Cheng,S.-C. (2021) Evidence for complex dynamics during U2 snRNP selection of the intron branchpoint. *Nucleic Acids Res.*, **49**, 9965–9977.
47. Yan,C., Wan,R., Bai,R., Huang,G. and Shi,Y. (2016) Structure of a yeast activated spliceosome at 3.5-Å resolution. *Science*, **353**, 904–911.
48. van Nues,R.W. and Beggs,J.D. (2001) Functional contacts with a range of splicing proteins suggest a central role for Brr2p in the dynamic control of the order of events in spliceosomes of *Saccharomyces cerevisiae*. *Genetics*, **157**, 1451–1467.

Received: June 30, 2023. **Revised:** September 3, 2023. **Editorial Decision:** September 5, 2023. **Accepted:** September 23, 2023